Experimental testing of two urban stressors on freshwater biofilms

Romain Vrba, Isabelle Lavoie, Nicolas Creusot, Mélissa Eon, Débora
Millan-Navarro, Agnès Feurtet-Mazel, Nicolas Mazzella, Aurélie Moreira,
Dolors Planas, Soizic Morin

HAL Id: hal-04613841
https://hal.inrae.fr/hal-04613841v1

Submitted on 17 Jun 2024

Experimental testing of two urban stressors on freshwater biofilms

Romain VRBA[1,2], Isabelle LAVOIE[2], Nicolas CREUSOT[1], Mélissa EON[1], Débora MILLAN-NAVARRO[1],
Agnès FEURTET-MAZEL[3], Nicolas MAZZELLA[1], Aurélie MOREIRA[1], Dolors PLANAS[4], Soizic MORIN[1*]

[1] INRAE, UR EABX, 50 avenue de Verdun, 33612 Cestas cedex, France
[2] INRS-ETE, 490 rue de la Couronne, Québec, QC G1K 9A9, Canada
[3] Univ. Bordeaux, UMR CNRS 5805 EPOC-OASU, F-336120 Arcachon, France
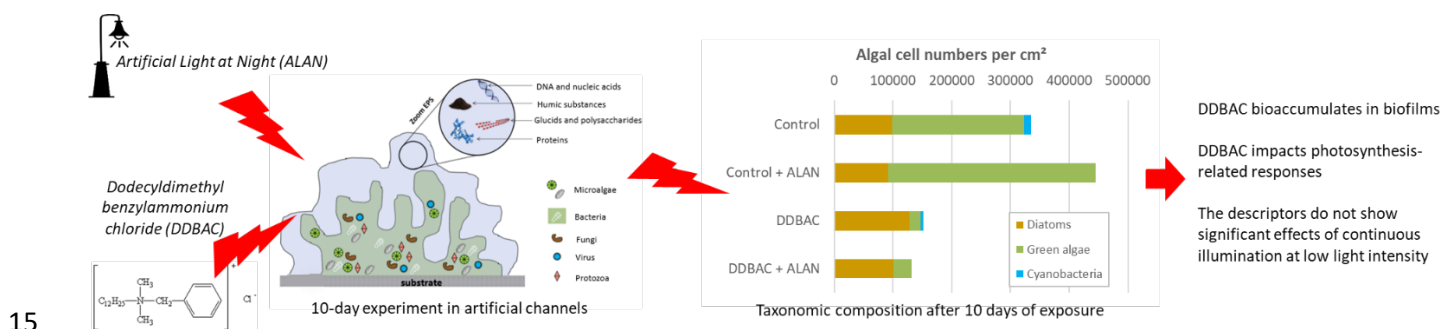[4] UQAM, GRIL-Département des sciences biologiques, 141 Avenue du Président-Kennedy, Montréal, QC H2X 1Y4, Canada
*Corresponding author at: INRAE, UR EABX, 50 avenue de Verdun, 33612 Cestas cedex, France.
Tel. : +33 6 95 43 84 28
E-mail address: soizic.morin@inrae.fr

Graphical abstract

Abstract

Aquatic ecosystems and their communities are exposed to numerous stressors of various natures (chemical and physical), whose impacts are often poorly documented. In urban areas, the use of biocides such as dodecyldimethylbenzylammonium chloride (DDBAC) and their subsequent release in wastewater result in their transfer to urban aquatic ecosystems. DDBAC is known to be toxic to most aquatic organisms. Artificial light at night (ALAN) is another stressor that is increasing globally, especially in urban areas. ALAN may have a negative impact on photosynthetic cycles of periphytic biofilms, which in turn may result in changes in their metabolic functioning. Moreover, studies suggest that exposure to artificial light could increase the biocidal effect of DDBAC on biofilms. The present study investigates the individual and combined effects of DDBAC and/or ALAN on the functioning and structure of photosynthetic biofilms. We exposed biofilms in artificial channels to a nominal concentration of 30 mg.L^{-1} of DDBAC and/or ALAN for 10 days. ALAN modified DDBAC exposure, decreasing concentrations in the water but not accumulation in biofilms. DDBAC had negative impacts on biofilm functioning and structure. Photosynthetic activity was inhibited by > 90% after 2 days of exposure, compared to the controls, and did not recover over the duration of the experiment. Biofilm composition was also impacted, with a marked decrease in green algae and the disappearance of microfauna under DDBAC exposure. The integrity of algal cells was compromised where DDBAC exposure altered the chloroplasts and chlorophyll content.

36 Impacts on autotrophs were also observed through a shift in lipid profiles, in particular a
37 strong decrease in glycolipid content was noted. We found no significant interactive effect of
38 ALAN and DDBAC on the studied endpoints.

39 **Keywords:** Biocide, ALAN, biofilm, photosynthetic efficiency, bioaccumulation, lipids.

1- Introduction

41 Biocides are widely used in different areas of activity including agriculture and industry, as
42 well as in a multitude of domestic products (e.g. pharmaceutical, personal care and household
43 products) (Abbott et al., 2020). Among these biocides, dodecyldimethylbenzylammonium
44 chloride (DDBAC) is commonly used as an active substance in medical disinfection products,
45 as well as in household products such as detergents. Recently, following the regulation of
46 some broadly used disinfectant agents such as triclosan, quaternary ammonium compounds
47 like DDBAC have become popular substitutes (Sreevidya et al., 2018; Arnold et al., 2023).
48 Moreover, DDBAC and all other benzalkonium chloride derivatives have been shown to be
49 very effective against the SARS-CoV virus (Rabenau et al., 2005), resulting in their widespread
50 use as disinfectants during the Covid 19 pandemic (US EPA, 2020). This multi-purpose product
51 eventually reaches wastewaters, where its concentration varies greatly depending on the land
52 use, population and wastewater treatment facilities, among other factors. For example, a
53 concentration of 6 mg.L^{-1} was recorded in hospital effluents (Kümmerer et al., 1997) due to
54 the intensive use of DDBAC as a disinfectant. In municipal wastewater effluents, DDBAC
55 concentrations were observed to range from just a few ng per liter up to 170 µg.L^{-1} (Clara et
56 al., 2007; Martínez-Carballo et al., 2007; Zhang et al., 2015).

57

58 Once in the aquatic environment, DDBAC is relatively stable to photodegradation and its half-
59 life in surface waters can reach 180 days, although the presence of photosensitizers (e.g.
60 natural organic matter, Hora & Arnold 2020, Mohapatra et al., 2024) can reduce this half-life
61 to a week (US EPA, 2006). The organic carbon-water partition coefficient (K$_{oc}$) of DDBAC is 5.43
62 and, therefore, it has a high adsorption ratio on sewage sludge, sediments or humic
63 substances (van Wijk et al., 2009). Although the transfer of DDBAC to urban aquatic
64 ecosystems has been recognized, the ecotoxicity of DDBAC is poorly documented. The toxicity
65 of DDBAC to cells is due to its quaternary ammonium polar head, which has the capacity to
66 bind to the surface membrane, while the alkyl lipophilic chain alters the phospholipid bilayer.
67 This alteration can rapidly lead to membrane disruption and progressive lysis of the cell (Eich
68 et al., 2000). Regarding aquatic organisms, there is redundancy in the biological models used
69 for toxicity assessment where most studies have focused on *Daphnia magna* to determine the
70 acute toxicity of DDBAC (Kreuzinger et al., 2007; Leal et al., 1994; Chen et al., 2014; Lavorgna
71 et al., 2016). To date, *D. magna* is the most sensitive organism to DDBAC, where the
72 concentration needed to immobilize 50% of organisms (EC$_{50}$) was of 5.9 µg.L^{-1} (US EPA, 2006).
73 As a result, the US EPA established a non-observed adverse effect concentration (NOAEC) of
74 4.15 µg.L^{-1} for aquatic invertebrates. Phytoplanktonic organisms seem to be less sensitive to
75 DDBAC than aquatic invertebrates. Indeed, other studies investigated the effects of DDBAC on
76 various microalgae species and the range of EC$_{50}$ based on growth was found to vary between

77 58 µg.L^{-1} for *Skeletonema costatum* (Kreuzinger et al., 2007) to 203 µg.L^{-1} for *Chlorella vulgaris*
78 (Sütterlin et al., 2008). However, to our knowledge, the chronic effects of DDBAC exposure on
79 natural aquatic communities has not been considered.

80

81 In this study, we focused on stream biofilms (periphyton), which are complex structures
82 housing autotrophic microorganisms (e.g. cyanobacteria, green algae, diatoms), bacteria,
83 fungi, and other heterotrophic organisms such as microfauna (Battin et al., 2016). Biofilms are
84 ubiquitous in aquatic environments, including urban streams and ponds. They form the basis
85 of aquatic food webs, providing a source of energy for primary producers, including essential
86 fatty acids (Brett and Müller-Navarra, 1997). Biofilms can also be found downstream of
87 wastewater treatment plants (WWTPs) and have been used as ecological indicators of stress
88 (Tamminen et al., 2022; Tlili et al., 2020). The early detection of ecosystem impairment using
89 autotrophic biofilms can be based on functional (e.g., photosynthesis) and structural
90 endpoints describing biodiversity based on taxonomy as well as pigments or lipid profiles
91 (Sabater et al., 2007; Morin & Artigas, in press). Biofilms are also efficient bioaccumulators of
92 organic substances carried by waters under dissolved or particulate forms (Bonnineau et al.,
93 2021). Given the toxic mode of action of DDBAC, impacts on biofilm fatty acids, particularly on
94 membrane phospholipids, are likely to occur. The attack on phospholipid membrane may also
95 result in the disruption of key functions of biofilm such as photosynthesis. For example, Pozo-
96 Antonio and Sanmartin (2018) showed a significant decrease in chlorophyll *a* and
97 photosynthetic efficiency of phototrophic biofilms from church walls after a DDBAC
98 treatment. The effect of DDBAC as a biofouling removal agent was significantly enhanced
99 when combined with artificial light or UV irradiation.

100

101 Artificial light at night (ALAN) has become a global pollution concern and, as of 2014, more
102 than 20% of the world's land surfaces between 75°N and 60°S were exposed to a light-polluted
103 sky (Falchi et al., 2016). Most urban areas have developed along rivers and coastlines,
104 increasing the exposure of urban aquatic environments to ALAN. Concerns about the impact
105 of ALAN on aquatic ecosystems and research on this topic are quite recent (Perkin et al., 2011).
106 Indeed, ALAN was only recognized as harmful for freshwater ecosystems in the early 2000s
107 (Longcore and Rich, 2004). ALAN could lead to disruptions in nycthemeral cycles of
108 autotrophic organisms in biofilms by inducing variability in the maximum efficiency of
109 photosynthesis (Maggi and Serôdio, 2020). ALAN can also alter taxonomic composition by
110 favouring certain autotrophic groups over others, thereby exerting differential selection, as
111 shown in a study where cyanobacteria proportions in biofilm decreased under ALAN (Grubisic
112 et al., 2017).

113

114 The objective of this study was to determine the individual and combined effects of two
115 anthropogenic stressors typical from urban aquatic ecosystems (DDBAC and ALAN) on
116 autotrophic organisms within biofilms, using structural and functional descriptors of impact.
117 To this aim, we performed a 10-day experiment in which natural autotrophic biofilms were
118 exposed in laboratory channels to DDBAC and/or ALAN. We hypothesized that, given the Koc

of the substance, DDBAC would bioaccumulate in the biofilms, generating toxicity to microorganisms. Functional (photosynthetic efficiency) and structural (taxonomic composition, pigment and lipid profiles) descriptors were predicted to be impacted by DDBAC exposure. ALAN was expected to modify the development of microalgae, thus to impact the proportions of algal groups, to alter photosynthetic efficiency to a certain extent, and to increase the sensitivity of microalgae to additional stress. As a consequence, we hypothesized that co-exposure to ALAN and DDBAC would enhance the toxic effects of the biocide.

## 2- Material and methods

2.1- Experimental design

Biofilms were grown in a DDBAC-free pond in Cestas, near Bordeaux, France. A previous study classified this small water body as a hypereutrophic pond (Chaumet et al., 2019; Neury-Ormanni et al., 2020). Glass slides (~200 cm²) were immersed in the photic zone, at a depth of 30-50 cm. Colonization took place in winter (December 2020 to April 2021), during five months to collect sufficient amounts of biomass. At this period, daylight irradiance on the top surface on the water (5 cm deep) was below 100 $\mu mol.s^{-1}.m^{-2}$. At the end of the colonization period, 36 glass slides covered by mature biofilms were randomly distributed among four series of experimental units (EU) for the experiment. The EUs consisted of experimental channels of about 30 L filled with pond water that had been previously filtered (20 µm) to remove suspended material and most planktonic organisms. To specifically assess the impacts of urban factors (DDBAC and ALAN), while avoiding possible inter-channel variability likely to influence biofilm responses,three parallel channels were set up and connected to individual 10-L tanks (one per EU, making the slides pseudoreplicates for each condition). Biofilms corresponding to day 0 (d0, 5 slides) were collected immediately after their recovery from the pond.

On d0, two EUs were contaminated with a solution of dodecyldimethylbenzylammonium chloride (DDBAC; Sigma Aldrich, France; CAS: 139-07-1, purity: >99%) to reach a concentration of 30 $mg.L^{-1}$. This concentration was selected to elicit an effect on photochemical efficiency while using as low a concentration as possible, based on the observed EC_5 of preliminary dose-response experiments (Appendix A). In order to assess only the effect of altered photoperiod, not light level, a non-stressful incident light intensity of 20 $\mu mol.s^{-1}.m^{-2}$ was selected. Light was kept on overnight and then from day 1 (d1), one control series and one DDBAC series were exposed to an alternating 14 h day / 10 h night photoperiod (alternated photoperiod, AP) and the other two series (one control, one DDBAC) were exposed to a 24 h day photoperiod (continuous photoperiod, CP) throughout the course of the experiment (Figure 1). Room temperature was maintained constant at 20.5 ± 0.1°C, while water temperature was kept at 18.7 ± 0.2°C. The tanks were refilled with 3 L of filtered pond water contaminated at 30 $mg.L^{-1}$ DDBAC on day 4 (d4) to compensate for water evaporation.
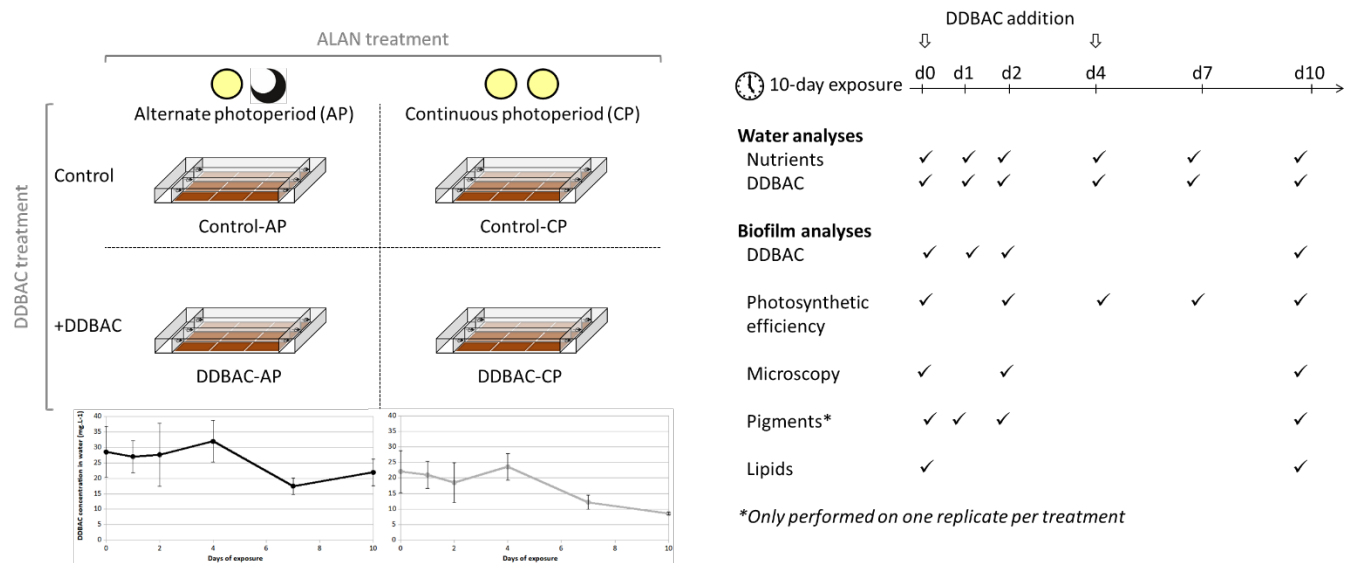
157
158 Figure 1: Experimental design and sampling strategy.

159

160 **2.2- Water chemistry measurements**

161 On d0, d1, d2, d4, d7 and d10, 20 mL water samples were taken from all channels, filtered on
162 1-µm PTFE filters and stored at 4°C in the dark until analysis (performed within 48 h of
163 collection). Nutrients and mineral salts were analysed as described in Chaumet et al. (2019),
164 using a Metrohm 881 Compact Ionic Chromatograph pro (Metrohm). Anion analysis (PO_4^-,
165 NO_3^-, NO_2^-, Cl^- and SO_4^{2-}) was performed using a Supp 4/5 Guard/4.0 precolumn followed by a
166 Metrosep A Supp5 – 250/4.0 column. The mobile phase was a mixture of a solution of 3.2
167 mmol.L^{-1} Na_2CO_3 and a solution of 1 mmol.L^{-1} $NaHCO_3$. Cation analysis (Na^+, K^+, Ca^{2+}, Mg^{2+} and
168 NH^{4+}) was performed using a C4 Guard/4.0 precolumn followed by a Metrosep C6 - 250/4.0
169 column). All precolumns and columns were provided by Metrohm. The eluent used was a
170 mixture of 2.5 mmol.L^{-1} HNO_3 and a solution of 1.7 mmol.L^{-1} 10,12-Pentacosadynoic acid
171 (PCDA). The limits of quantification (LOQ) of the different ions analysed are shown in Table 1.

172 DDBAC concentrations in the water were monitored frequently over the experiment, at d0,
173 d1, d2, d4, d7 and d10. Three samples of 20 mL were collected from each channel and stored
174 at -20°C together with the stock solution until analysis. The samples were analysed using an
175 Ultimate 3000 HPLC coupled with an API 2000 triple quadrupole mass spectrometer. We used
176 a Gemini® NX-C18 column from Phenomenex as a stationary phase. The mobile phase was
177 90:10 5 mM ammonium acetate/acetonitrile. We worked in isocratic mode, so the
178 composition of the mobile phase was constant during the analysis. The flow rate was set at
179 0.6 mL.min^{-1} and the injection volume was set at 20 µL. An internal standard of benzyl-
180 2,3,4,5,6-d5-dimethyl-n-dodecylammonium chloride (DDBAC-d5) was used (Cluzeau, France;
181 CAS: 139-07-1, purity: >98%) at an equivalent of 100 µg.L^{-1} in both samples and standard
182 solutions for calibration. The mass spectrometer was operated in multiple reaction monitoring
183 (MRM) mode with a total cycle time of 0.8 seconds. The MRM transitions were 304>91
184 (quantitation) and 304>212 (confirmation) for DDBAC. For DDBAC-d5, the MRM transitions
185 were 309>96 and 309>212. The declustering potential was set to 65 V and the collision

186 energies were set either to 45 or 30 V for the quantitation or confirmation transition,
187 respectively. Samples were diluted and the calibration range was from 1 to 200 µg.L^{-1}. Quality
188 controls were regularly injected at concentrations of 5 and 25 µg.L^{-1}, as well as analytical
189 blanks.

190

191 **2.3- Biofilm biological endpoints**
192 *2.3.1- Photosynthetic efficiency*

193 We sampled 2 cm² of biofilm from three different glass slides for each treatment on d0, d2,
194 d4, d7, and d10, corresponding to three pseudoreplicates per treatment per sampling. Each
195 biofilm sample was then suspended in 3 mL of channel water and gently shaken for
196 homogenization. Photosynthetic activity (effective photosystem II quantum yield) was
197 assessed on suspensions of biofilm (Genty et al. 1989) within one hour after collection using
198 a Pulse Amplitude Modulation fluorimeter (Phyto-PAM, Heinz Walz GmbH, Germany) in
199 quartz cuvettes under continuous agitation (Emitter–Detector Unit PHYTO-ED). Biofilm
200 suspensions were adapted for 15 min to light (164 µmol.m^{-2}.s^{-1}) before fluorescence
201 measurements at the same active radiation, in Actinic Light mode. The quantum yield values
202 reported are mean values of five measurements per replicate, averaged for the three pigment
203 groups using the device's reference spectra. After photochemical efficiency measurements,
204 samples were preserved for further microscopic analyses by adding a few drops of Lugol
205 solution then stored in the dark at 4°C.

206 *2.3.2- Microscopic analyses*

207 For microscopic observations, a Nageotte counting slide (Marienfeld, Germany) was used with
208 125 µL biofilm suspension samples collected on d0, d2 and d10 to determine initial taxonomic
209 composition as well as to assess early structural changes and chronic effects of ALAN and
210 DDBAC. Observations were made at x400 magnification under an optical microscope
211 (Olympus BX51) equipped with a digital camera as described in Morin et al. (2010). Ten fields
212 of view were scanned for enumeration of the main taxonomic groups observable on preserved
213 material: diatoms, green algae, cyanobacteria and microfauna. Solitary and colonial algae and
214 cyanobacteria were recorded and counted as cell numbers to allow for density comparisons.
215 Microfauna organisms were recorded as individuals. All densities were expressed as a function
216 of colonized biofilm surface (i.e., per cm²). Live (intact cell content) and dead (empty frustules)
217 diatoms were counted separately to estimate mortality (Morin et al. 2010).

218 *2.3.3- Analyses from freeze-dried biofilms*

219 Biofilms were scraped from glass slides on d0, d1, d2 and d10 (4 slides per treatment) and
220 were frozen in liquid nitrogen to prevent lipid degradation. The samples were then lyophilized
221 for 24 hours, and used to determine lipid content, DDBAC bioaccumulation, and
222 concentrations of photosynthetic pigments. Analyses focused on neutral lipids (storage lipids:
223 triacylglycerides) and on polar lipids. Polar lipids correspond to phospholipids (lipids typical
224 from cytoplasmic membranes: phosphatidylcholine-PC, phosphatidylethanolamine-PE, and
225 phosphatidylglycerol-PG) and to glycolipids (characteristic from chloroplastic membranes:

226 digalactosyldiacylglycerol-DGDG,   monogalactosyldiacylglycerol-MGDG,
227 sulfoquinovosyldiacylglycerol-SQDG). Lipids were extracted from the biofilms (20 mg dry
228 weight) using a mixture of MTBE-methanol (3:1 %v/v) and UPW-methanol (3:1 %v/v) with 150
229 mg of microbeads. Samples were then homogenized using a FastPrep (MP Biomedicals). The
230 upper organic fraction of the samples (i.e. MTBE) was recovered by centrifugation for lipid
231 analysis, while the lower hydrophilic fraction (mixture of UPW and methanol) was used to
232 determine DDBAC bioaccumulation.

2.3.3.1- Lipid quantification

234 For lipid analysis, samples from d0 and d10 were evaporated and injection solvent was added
235 before analysis by HPLC-MS/MS following the protocol detailed in Mazzella et al. (2023a).
236 Briefly, different stationary and mobile phases were used for the analysis of
237 phospholipids/glycolipids and triglycerides. For the phospholipid and glycolipid analyses, a
238 LUNA® NH2 HILIC column (100 x 2 mm, 3 μm) from Phenomenex was used as the stationary
239 phase, and a mixture of acetonitrile and 40 mM ammonium acetate buffer as the mobile
240 phase. The flow rate was set at 400 μL.min^{-1}. The proportions of these two solutions are given
241 in Appendix C. For the analysis of triglycerides and betaine lipids (i.e.
242 diacylglyceryltrimethylhomo-Ser, DGTS), a KINETEX® C8 column (100 x 2.1 mm, 2.6 μm) from
243 Phenomenex was used as the stationary phase, and the mobile phase was a mix of a solution
244 of acetonitrile/water/40 mM ammonium acetate buffer (600/390/10, v/v/v) and a solution of
245 isopropanol/acetonitrile/1 M ammonium acetate buffer (900/90/10, v/v/v). The flow rate was
246 set at 300 μL.min^{-1}. The proportions of these two solutions are given in Appendix C. Results
247 were then pre-treated with ANALYST® 1.6.2 software from Sciex. For polar lipids (i.e.
248 glycolipids and phospholipids), the limits of quantification ranged from 0.1 to 0.5 nmol.mg^{-1},
249 depending on the lipid classes. For triglycerides and DGTS, the limits of quantification reached
250 were 0.01 and 0.1 nmol.mg^{-1}, respectively. Results were expressed as nmol.g^{-1} freeze-dried
251 biofilm.

2.3.3.2- DDBAC accumulation in biofilms

253 The same analytical method used for water samples was used to determine bioaccumulated
254 DDBAC in the previously extracted hydrophilic fraction. It was generally necessary to perform
255 significant dilutions (i.e. 10,000-fold) in order to stay within the calibration range. Results were
256 then expressed in the log10 value of the bioconcentration factor (i.e. log(BCF)). The BCF was
257 calculated according to the following formula:

258 $$BCF = \frac{Concentration\ of\ DDBAC\ in\ biofilm\ (mg.kg^{-1})}{Concentration\ of\ DDBAC\ in\ water\ (mg.L^{-1})} \text{(Eq.1)}$$

2.3.3.3- Photosynthetic pigments

260 On selected freeze-dried samples (one replicate per treatment), pigment analyses were also
261 performed following the French standard NF T90-117 (1999). Ten mg of dry biofilm were put
262 in solution using 10 mL of acetone. After 20 minutes of ultrasonication, the mix was filtered
263 on a Büchner filter to remove the solid phase. Absorption was measured at the wavelengths
264 630 nm, 647 nm, 664 nm, 665 nm and 750 nm with a UV-1800 (Shimadzu) spectrophotometer,
265 and was then remeasured at the same wavelengths after acidification of the samples. The

266 concentrations of chlorophyll pigments and phaeopigments were determined following the
267 equations of Lorenzen (1967) and expressed as µg pigments.mg^{-1} freeze-dried biofilm.

268

269 **2.4-   Data analyses**

270 ANOVAs were performed after verification that homogeneity of variances and normality were
271 met. A one-way ANOVA was used to test the effect of ALAN on DDBAC degradation, and two-
272 way ANOVAs were used to assess the individual effect of ALAN and DDBAC, as well as their
273 interaction, on nutrient concentrations. Two-way ANOVAs with sampling dates as repeated
274 measures were conducted to assess the individual and interactive effects of ALAN and DDBAC
275 (categorical variables with 2 levels: yes/no) on biofilm endpoints. . Data were processed using
276 R software (R Core Team, 2022).

3- Results

3.1- Water chemistry

Table 1. Principal ions and DDBAC concentrations (mg.L^{-1}) in the four experimental treatments along the ten days of exposure. Results are expressed as the mean and standard error for the whole experiment. Two-way ANOVAs were conducted, with ALAN and DDBAC as the two factors, except for DDBAC concentrations (One-way ANOVA assessing the effect of ALAN). DDBAC = contaminated biofilm; Control = non-exposed biofilm; AP = alternated photoperiod; CP = continuous photoperiod; LOQ = Limit of quantification.

| Treatment	DDBAC	NO$_2^-$	NO$_3^-$	PO$_4^{3-}$	SO$_4^{2-}$	Cl$^-$	NH$_4^+$	Na$^+$	K$^+$	Ca^{2+}	Mg^{2+}
Control-AP	<LOQ	0.04 ± 0.03	1.69 ± 0.27	0.03 ± 0.02	21.0 ± 1.8	36.4 ± 2.7	0.09 ± 0.05	22.0 ± 1.9	4.80 ± 0.43	57.8 ± 5.1	4.90 ± 0.42
DDBAC-AP	26.6 ± 2.5	0.02 ± 0.00	0.66 ± 0.17	0.03 ± 0.02	18.9 ± 0.8	35.5 ± 1.4	0.11 ± 0.05	19.7 ± 0.9	4.34 ± 0.20	52.2 ± 2.5	4.41 ± 0.20
Control-CP	<LOQ	0.02 ± 0.01	1.35 ± 0.23	0.01 ± 0.00	17.5 ± 0.3	30.3 ± 0.4	0.09 ± 0.06	18.5 ± 0.3	4.12 ± 0.06	48.4 ± 0.6	4.09 ± 0.06
DDBAC-CP	18.5 ± 2.0	0.02 ± 0.00	0.75 ± 0.10	0.03 ± 0.02	17.8 ± 0.3	33.0 ± 0.6	0.10 ± 0.06	18.8 ± 0.9	4.21 ± 0.11	49.5 ± 1.2	4.18 ± 0.09
LOQ	0.001	0.005	0.01	0.01	0.005	0.01	0.005	0.01	0.0025	0.15	0.15
Significant factor(s) and interaction(s)	ALAN	None	DDBAC	NA	DDBAC	DDBAC	NA	DDBAC	NA	DDBAC	DDBAC
p	<0.001	>0.05	<0.001	NA	<0.05	<0.01	NA	<0.05	NA	<0.05	<0.05

284 In the control channels, DDBAC concentrations were always below quantification limit (Table
285 1), confirming that no cross-contamination occurred. Contaminant concentrations averaged
286 26.6 ± 2.5 mg.L^{-1} (AP) and 18.5 ± 2.0 mg.L^{-1} (CP) in the DDBAC treatments. Differences in
287 DDBAC concentrations were observed between the DDBAC treatment channels exposed to an
288 alternated photoperiod and those exposed to a continuous photoperiod ($F_{[1,10]}$ = 232.72; p <
289 0.001, also see Figure 1), suggesting that degradation occurred under continuous
290 photoperiod. Nutrient concentrations were also modified by DDBAC exposure (Table 1).
291 Indeed, DDBAC addition resulted in lower concentrations of nitrate, sulfate, Cl$^-$, Na$^+$, Ca^{2+} and
292 Mg$^+$ than in the control (Table 1), while ALAN showed no effect on nutrient concentrations.

293

294 **3.2- Bioaccumulation of DDBAC in biofilms**

295 **Figure 2. Evolution of DDBAC bioaccumulated in biofilms (expressed in log(BCF)) between the different**
296 **ALAN treatments (n=3). AP = alternated photoperiod CP = continuous photoperiod**
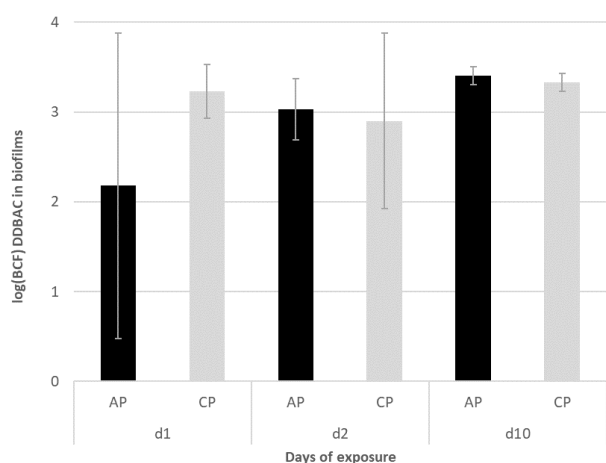
297

298 Figure 2 shows the log(BCF) for the hydrophilic fraction of biofilm samples at d1, d2 and d10
299 for AP and CP treatments. DDBAC was recovered from biofilms for every treatment and every
300 sampling time, showing that this compound bioaccumulates well in autotrophic biofilms, with
301 a mean log(BCF) of 3.22 ± 0.25. The amount of DDBAC bioaccumulated in the biofilms showed
302 no significant changes between sampling times ($F_{[2,28]}$= 2.38; p = 0.11) nor ALAN treatments
303 ($F_{[1,28]}$ = 0.28; p = 0.60), and no Time x ALAN interaction ($F_{[2,28]}$ = 0.025; p = 0.98).

304

305 **3.3- Photosynthetic efficiency**

306
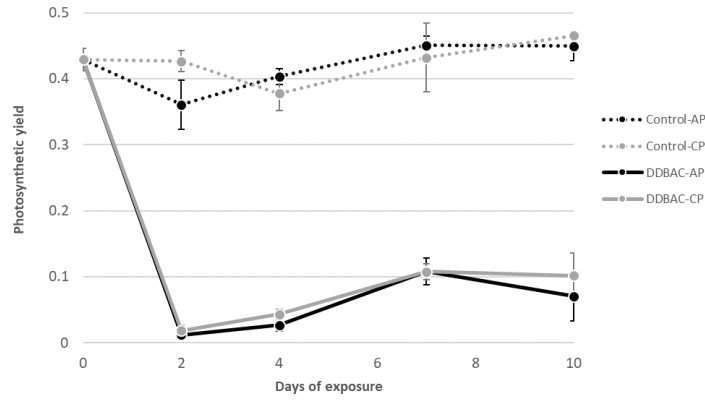
308 **Figure 3. Evolution of photosynthesis yield in biofilms along the ten days of the experiment (d0: n=5, d2 and**
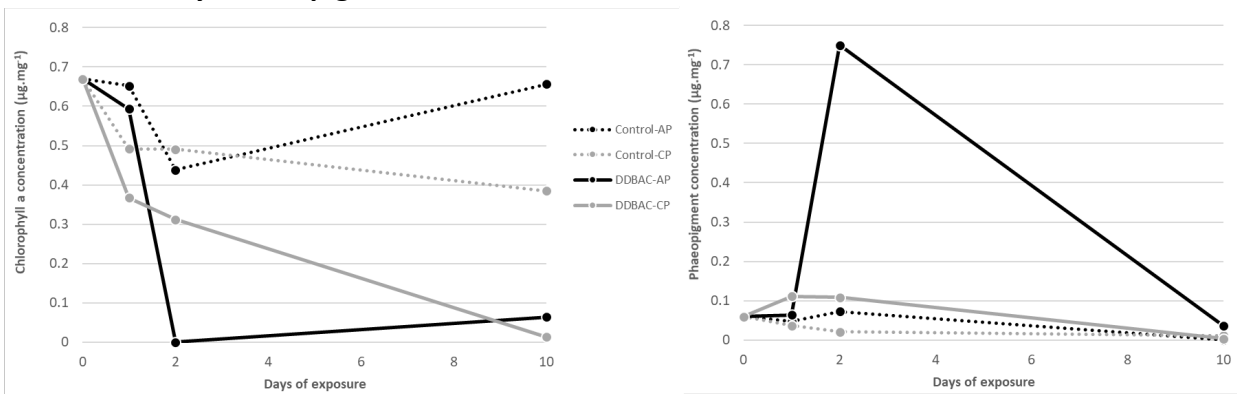309 **d10: n=3). Control = non-exposed biofilm; DDBAC = contaminated biofilm; AP = Alternated**
310 **Photoperiod; CP = Continuous Photoperiod**

Figure 3 shows that photosynthetic activity was stable over the time of the experiment, with a mean value of 0.42 ± 0.01 in the control AP and CP channels, regardless of the ALAN treatment ($F_{[1,42]}$ = 2.65; p > 0.05). Biofilms exposed to DDBAC showed an almost complete inhibition of photosynthetic yield starting from d2 and lasting until the end of the experiment ($F_{[1,42]}$ = 1279; p < 0.001). In the same way as for control channels, photosynthetic activity showed no difference between AP and CP for contaminated channels ($F_{[1,42]}$ = 0.18; p = 0.67).

3.4- Photosynthetic pigments

321 **Figure 4. Changes in photosynthetic pigments content in biofilms along the ten days of the experiment (n =**
322 **1). Control = non-exposed biofilm; DDBAC = contaminated biofilm; AP = alternated photoperiod; CP =**
323 **continuous photoperiod.**

Chlorophyll *a* concentrations decreased over time in the DDBAC contaminated samples, compared to the control samples (Figure 4). At d2, no chlorophyll *a* was detected in the DDBAC-AP samples, and only phaeopigments were measured. At the end of the experiment, pigment concentrations in DDBAC samples were very low compared to the controls. Unfortunately, the lack of replication does not allow for any conclusion on the effect of the tested treatments on chlorophyll *a* or phaeopigments.

333 **3.5- Community composition**

334

Table 2. Evolution of the taxonomic composition of biofilms during the experiment. Densities are expressed as individuals×10^3 / cm², i.e. number of cells for microalgae, and number of organisms for microfauna. Diatom mortality is expressed in %. Results are expressed as mean and standard error for each date and treatment (d0: n=5, d2 and d10: n=3). DDBAC = contaminated biofilm; Control = non-exposed biofilm; AP = Alternated Photoperiod; CP = Continuous Photoperiod

335

Date	Treatment	Diatom density	Diatom mortality	Green algae density	Cyanobacteria density	Microfauna density
d0	Control	81.3 ± 33.7	7 ± 1	4.1 ± 2.3	3.8 ± 2.0	0.3 ± 0.0
d2	Control-AP	141.3 ± 9.1	3 ± 0	26.7 ± 4.4	1.6 ± 2.0	0.6 ± 0.3
d2	DDBAC-AP	113.2 ± 11.5	3 ± 1	11.8 ± 2.8	0	0.2 ± 0.2
d2	Control-CP	132.1 ± 68.8	3 ± 1	51.7 ± 46.0	0	0.3 ± 0.3
d2	DDBAC-CP	145.0 ± 26.1	2 ± 1	6.2 ± 1.7	0	0
d10	Control-AP	98.2 ± 11.7	5 ± 2	225.6 ± 133.5	11.2 ± 7.8	0.9 ± 0.5
d10	DDBAC-AP	128.5 ± 26.0	2 ± 0	18.9 ± 15.0	4.8 ± 3.0	0
d10	Control-CP	91.3 ± 14.2	6 ± 1	354.2± 83.1	0	1.0 ± 0.2
d10	DDBAC-CP	101.0 ± 27.0	1 ± 0	30.7 ± 8.2	0	0
	Significant factor(s) and interaction(s)	None	DDBAC	DDBAC × Time	None	DDBAC × Time
	p	>0.05	<0.05	<0.001	>0.05	<0.01

336

337 Diatoms (91%) dominated the biofilm community at d0, whereas low proportions of green
338 algae (5%), cyanobacteria (4%) and microfauna (1%) were observed (Table 2). In the control
339 channels, green algae developed markedly and became the main algal group in terms of
340 density by d10, with no significant effect of the ALAN treatment (e.g. 67% in AP channels and
341 79% in CP). The density of green algae slightly increased from d0 to d10 in the DDBAC
342 contaminated channels, but not to the same extent as in the control channels. Indeed, a
343 significant Time × DDBAC interaction was highlighted for green algae densities (p < 0.001;

344 Table 2). Microfauna increased in control channels, but had completely disappeared from
345 biofilms exposed to DDBAC by d10. For this component, a significant Time × DDBAC interaction
346 was also noted (p < 0.01; Table 2). ALAN treatments did not have a significant impact on the
347 biofilm taxonomic composition.

348 Diatom mortality values (based on the ratio between frustules without cell content and total
349 diatom frustules) significantly decreased under DDBAC exposure (Table 2). In addition,
350 microscopic observations highlighted differences in the aspect (shape, colour) of chloroplasts
351 in diatoms and chlorophytes exposed to DDBAC, becoming highly granular and darker (Figure
352 B.2). These were, however, not considered as 'dead' cells in estimating diatom mortality.
353

354

355 **3.6- Lipid content**

356
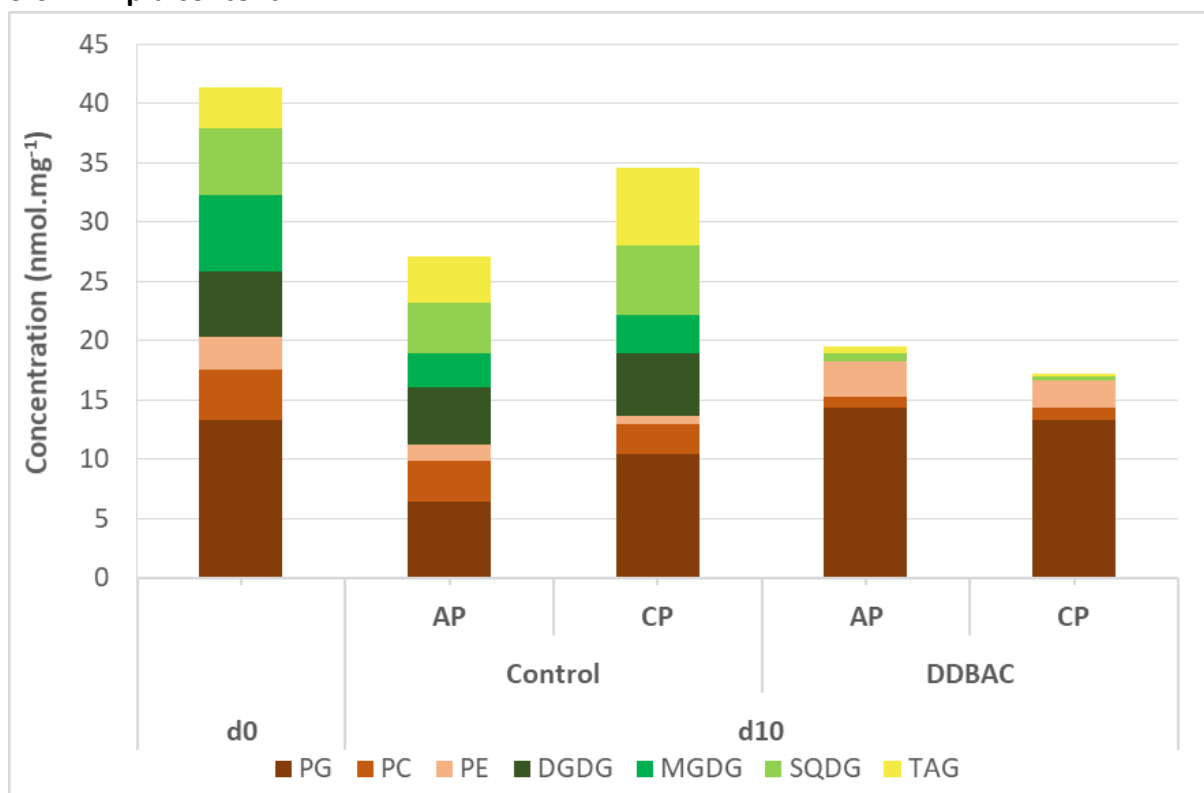
Figure 5. Effects of DDBAC and continuous photoperiod on the proportion of total lipids and on lipid classes (n=4). DDBAC = contaminated biofilm; Control = non-exposed biofilm; AP = alternated photoperiod; CP = continuous photoperiod; PE = phosphatidylethanolamine; PC = phosphatidylcholine; PG = phosphatidylglycerol; DGDG = digalactosyldiacylglycerol; MGDG = monogalactosyldiacylglycerol; SQDG = sulfoquinovosyldiacylglycerol; TAG = triacylglycerides.

362

363 On d0, total lipid concentration reached 42.6 nmol.mg^{-1} of biofilm dry weight. Almost half of
364 the lipids were phospholipids, and the other half were glycolipids, while neutral lipids (TAG)
365 represented a minor portion (Table 3). By d10, total lipid concentration had decreased in all
366 treatments down to an average of 23.6 ± 7.53 nmol.mg^{-1} of biofilm dry weight (Table 3). No
367 significant differences were found between AP and CP, while DDBAC significantly affected

368 glycolipids over time (significant Time × DDBAC interaction; p < 0.01). Figure 5 shows lipid
369 contents under DDBAC and ALAN exposure on d0 and d10. At the beginning of the experiment,
370 phosphatidylglycerol (PG) was the predominant lipid in the biofilms, while phospholipids and
371 glycolipids in the biofilms were evenly distributed. Total lipid amounts decreased over time in
372 the controls, but the proportions of phospholipids and glycolipids remained similar to those
373 at d0, all the main classes of lipids being present. Total phospholipids remained stable over
374 time, whatever the treatment (p > 0.05), but phoshatidylethanolamine (PE) and PG were
375 higher in biofilms exposed to DDBAC compared to controls (Figure 5, Table 3). In the samples
376 exposed to DDBAC, glycolipids such as monogalactosyldiacylglycerol (MGDG) and
377 digalactosyldiacylglycerol (DGDG) decreased significantly, or even became barely detectable,
378 with significant Time × DDBAC interactions (respectively, p < 0.01 and 0.001).
379 Diacylglyceryltrimethylhomo-Ser (DGTS) was never detected and, therefore, is not mentioned
380 further.

Table 3: Evolution of lipid content of biofilms (in nmol.g-1 freeze-dried biofilm) between the beginning and the end of the experiment. Results are expressed as mean and standard error for each date and treatment (n=4). DDBAC = contaminated biofilm; Control = non-exposed biofilm; AP = Alternated Photoperiod; CP = Continuous Photoperiod; PE = phosphatidylethanolamine; PC = phosphatidylcholine; PG = phosphatidylglycerol; DGDG = digalactosyldiacylglycerol; MGDG = monogalactosyldiacylglycerol; SQDG = sulfoquinovosyldiacylglycerol; TAG = triacylglycerides. Two-ways ANOVAs on repeated measures were applied on data.

381

Date	Treatment	Neutral lipids (TAG)	PG	PE	PC	Σ Phospholipids	DGDG	MGDG	SQDG	Σ Glycolipids	Total lipids
d0	Control	4.2 ± 2.5	13.7 ± 3.1	2.8 ± 0.5	4.6 ± 0.2	21.0 ± 3.3	5.6 ± 1.2	6.4 ± 1.6	5.3 ± 1.1	17.3 ± 2.4	42.6 ± 3.2
d10	Control-AP	3.9 ± 2.0	6.4 ± 1.0	1.3 ± 0.5	3.5 ± 1.5	11.2 ± 2.4	4.8 ± 0.8	2.9 ± 0.5	4.2 ± 0.7	12.0 ± 0.4	27.1 ± 4.1
d10	DDBAC-AP	0.2 ± 0.3	14.3 ± 2.6	3.0 ± 0.4	0.9 ± 0.4	18.2 ± 2.6	0	0	0.7 ± 0.2	0.7 ± 0.2	19.1 ± 2.6
d10	Control-CP	6.6 ± 2.9	6.9 ± 6.7	0.7 ± 0.1	2.6 ± 1.1	10.1 ± 7.8	5.3 ± 0.2	3.3 ± 1.1	5.8 ± 1.2	14.4 ± 2.2	31.1 ± 8.1
d10	DDBAC-CP	0.1 ± 0.1	13.3 ± 3.5	2.3 ± 1.0	1.0 ± 1.0	16.6 ± 5.2	0	0	0.4 ± 0.2	0.4 ± 0.2	17.1 ± 5.3
	Significant factor(s)	DDBAC × Time	DDBAC × Time	DDBAC × Time	DDBAC × Time	None	DDBAC 12× Time	DDBAC × Time	DDBAC × Time	DDBAC × Time	DDBAC × Time
	p	0.01	<0.05	<0.01	<0.01	>0.05	<0.001	<0.01	<0.001	<0.001	<0.001

382

15

4. Discussion

4.1- Experimental conditions and DDBAC exposure

In this experiment, natural biofilms were transferred to controlled laboratory conditions under ALAN and DDBAC treatments. Changes in environmental conditions were likely to affect biofilm characteristics; control conditions were however favourable to the development of autotrophic biofilms, as highlighted by continuous growth from d0 to d10 and by stable physiological state (assessed through photosynthetic efficiency). During the 10 days, most physicochemical parameters remained stable, and no nutrient depletion was observed at the end of the experiment in any treatment. However, DDBAC seemed to have an indirect effect on the concentrations of certain nutrients over the 10-day exposure period of our experiment. For example, under DDBAC exposure, concentrations of NO_3^- were lower than in the control (Table 1).

Contrary to the hypothesis of Pozo-Antonio and Sanmartin (2018), who suggested that artificial light could lead to an increase in internalization of the contaminant, we found no significant difference in DDBAC concentrations in biofilm between ALAN treatments (Figure 2). Thus, our results do not support the hypothesis of a higher uptake of the substance from the water through increased bioaccumulation under ALAN exposure. Lower concentrations of DDBAC under CP compared to AP (Figure 1) might be linked to the differential development of microorganisms exposed to ALAN. Some bacterial strains such as *Aeromonas hydrophila* can biodegrade DDBAC under N-depleted conditions and use the degradation product as a source of nitrogen (Patrauchan and Oriel, 2003). The above-mentioned decrease in certain nutrient concentrations in the water under DDBAC treatment may have provided favourable conditions for such strains able to grow consuming DDBAC as a nutrient source. Moreover, the low light intensity used in the experiment may have enhanced the growth of such heterotrophs in the absence of a strong competition with autotroph organisms from the biofilm..

The potential for DDBAC exposure on biofilm consumers (related to bioaccumulation in the biofilm) was similar between ALAN treatments, independently of differences in DDBAC concentrations in the water. DDBAC accumulation rapidly stabilized to average log(BCF) of 3.22 (Figure 2), falling in the range measured for organochlorine substances in biofilms, and greater than previous observations for other pesticides or pharmaceuticals (Bonnineau et al. 2021). Our results demonstrate the retention capacity of biofilms for this compound, suggesting a risk of transfer to primary consumers.

4.2- Effects of DDBAC on the biofilm

The first effect of DDBAC observed was the marked and rapid decrease in photosynthetic efficiency (more than 90% compared with the initial yield; Figure 3). This sudden inhibition of photosynthesis was not expected because the exposure concentration was based on the EC_5 for photosynthesis inhibition after four hours of exposure determined in a preliminary experiment ($EC_5 = 30$ mg.L^{-1}; Figure A). However, this result is in line with the high ecotoxicity of DDBAC to freshwater and estuarine/marine algae reported by Arnold et al. (2023), with EC_{50} values as low as 14 μg.L^{-1}. Based on our microscopic observations, diatom mortality was low in all samples (<10%). It should be noted that, following Morin et al. (2010), only diatoms that

426   no longer had chlorophyll in their cell content were considered as dead cells, while cells with
427   chloroplasts were counted as live diatoms. However, many of the cells where chloroplastic
428   content was observed seemed to have suffered critical alteration of their photosynthetic
429   equipment (Figure B.2). Their integrity was potentially severely affected, which could explain
430   the loss of photosynthetic yield in biofilms exposed to DDBAC. This deterioration of cell
431   integrity may be due to the fact that DDBAC is able to quickly penetrate the cell (Severina et
432   al. 2001). Our results highlight, in agreement with Wood et al. (2014) and Pandey et al. (2017),
433   the ecological relevance of microscopic observations of fresh material to better assess the
434   ecotoxicity of biocides.

435   Marked differences in the autotrophic community composition were highlighted by
436   microscopy counts between d2 and d10 under DDBAC exposure. Indeed, densities of green
437   algae were 10 times lower than under control conditions (Table 2). Despite the lack of
438   replication for pigment analyses, the degradation of chlorophyll pigments in DDBAC
439   treatments (Figure 4) is in line with the impairment of the algal component of the biofilms as
440   highlighted through photosynthetic inhibition and chloroplast alteration. The striking
441   decrease in lipid content in biofilms exposed to DDBAC (Table 3), particularly glycolipids found
442   mainly in thylakoid membranes within photosynthetic cells (Zulu et al., 2018), supports the
443   idea that the contaminant is internalized within phototrophic cells, with deleterious impacts
444   on the autotrophic component. Diatom-rich biofilms are generally source of essential
445   polyunsaturated fatty acids such as eicosapentaenoic acid (Zulu et al., 2018), ensuring a high
446   nutritional quality of this food resource for primary consumers (Brett and Müller-Navarra,
447   1997). Demailly et al. (2019) also demonstrated that diatom fatty acid composition may be
448   altered by organic substances such as pesticides. More recently, Mazzella et al. (2023b)
449   highlighted a decrease in eicosapentaenoic acid content, and more generally in
450   polyinsaturated fatty acids, in DDBAC-exposed biofilms collected from the present study.
451   DDBAC-driven changes in biofilm community structure and impact on glycolipids could
452   therefore lead to a decrease in the nutritional quality of biofilms (decrease in essential
453   polyunsaturated fatty acids, such as certain omega-3 and omega-6) and subsequently affect
454   the trophic chain (Brett and Müller-Navarra, 1997), worsened by DDBAC accumulation.

455   In parallel to the decrease in glycolipids noted under DDBAC contamination, we observed an
456   increase in phospholipids. It is difficult to clearly explain this increase because the
457   phospholipid groups analysed (i.e. PE, PC and PG) are not specific to any taxonomic group and
458   can be found in both the plasma membranes of microalgae (Zulu et al., 2018) and in
459   prokaryotic cells (Li-Beisson et al., 2013). One hypothesis to explain this increase could be the
460   development of DDBAC-resistant bacteria, as mentioned above. Indeed, the mechanism of
461   resistance to benzalkonium chloride identified in *Pseudomonas aeruginosa* consists of an
462   increase in the percentage of phospholipids (Sakagami et al. 1989). Considering the impact of
463   DDBAC on biofilm bacteria would be required to determine if the increase in phospholipids
464   observed in our study reflects the development of specific bacteria under DDBAC exposure.

465   Sensitivity to DDBAC differed among biofilm taxa, whose proportions changed over time, and
466   with DDBAC concentration. This result suggests that the biofilm community acclimated to the
467   chemical stress and that only resistant/tolerant species survived DDBAC exposure according

to the Pollution-Induced Community Tolerance concept (Blanck et al., 1988). Diatoms appeared to be minimally affected based on growth and mortality, even though the alteration of their photosynthetic structure and cell content suggests a marked impact (Figure B.2). Green algae, which experienced rapid growth in non-contaminated channels, appeared to be negatively affected by DDBAC at d10. DDBAC also had a strong effect on heterotrophic microfauna naturally present in the biofilms (e.g. rotifers), suggesting that they are highly sensitive to this contaminant. Our dataset does not allow to disentangle whether such impacts derive from direct (through water contamination) or indirect (trophic transfer from contaminated biofilms) effects. However, such results confirm the high sensitivity of aquatic microfauna and invertebrates to DDBAC, as already demonstrated for acute exposure with *Daphnia magna* (Kreuzinger et al., 2007; Leal et al., 1994; Chen et al., 2014; Lavorgna et al., 2016).

4.3- Effects of ALAN on the biofilm

Our experimental conditions were based on constant light intensities over time, which does not represent realistic conditions. In the field, daylight variations in irradiation are important drivers of biofilm growth and photosynthetic performance (Laviale et al. 2009). Under our exposure conditions, ALAN did not significantly modify the structure or physiology of the autotrophic organisms in the biofilm based on the parameters that we investigated. The low light intensity chosen, and the use of similar light levels during day and night, may have not been enough to generate stress during continuous light exposure, at the timescale of the experiment. Indeed, using biofilms originating from the same pond and exposed to higher irradiance (~200 $\mu mol.s^{-1}.m^{-2}$), Roux et al. (2024) highlighted than ALAN decreased the daily photosynthetic yield after 14 and 30 days of exposure.

Concerning the polar lipid classes, an increase in MGDG or DGDG is often observed during low light intensity exposures (Gushina and Harwood, 2009). In the present experiment, while light was low, the duration of exposure differed, which could explain the absence of a significant effect on these two glycolipids over time. Conversely, high light levels can lead to a decrease in polar lipids, especially phospholipids, in favour of TAGs, especially in the case of filamentous green algae such as *Cladophora* spp. (Gushina and Harwood, 2009). Changes in lipid content with ALAN were not clearly observed here, contrarily to what was observed based on a more detailed assessment of fatty acids conducted on the same samples (Mazzella et al. (2023b). Amini Khoeyi et al. (2011) also showed that a prolonged photoperiod can decrease the content of monounsaturated (MUFA) and polyunsaturated (PUFA) fatty acids in the microalgae *Chlorella vulgaris*. Considering the constant low light conditions we used, it is likely that the apical endpoints we measured did not allow to observe subtle changes occurring at the individual or subindividual scales. This could be due to compensation phenomena or to the fact that we averaged lipids across different organisms present within a natural biofilm, which differs from the analysis of an isolated chlorophyte strain.

4.4- Combined effects of DDBAC and ALAN on the biofilm

509 Contrary to our hypotheses, DDBAC and ALAN exposure did not show interaction effects on
510 any of the biological endpoints monitored in this experiment. However, ALAN impacted the
511 fate of DDBAC by decreasing exposure concentrations in the medium under our experimental
512 conditions. This result can hardly be extrapolated to natural light regime conditions, calling for
513 further investigations under more realistic light scenarios. DDBAC exposure caused significant
514 impacts on biofilm function and structure, especially impacting autotrophs. Given the wide
515 range of uses of DDBAC, our study highlights that its transfer to the aquatic environment may
516 result in a significant impairment of the functioning of aquatic ecosystems. As the high
517 concentration of DDBAC tested drove most of the changes observed in biofilm composition
518 and physiology, we cannot exclude that DDBAC exposure masked possible interactions with
519 ALAN. Further experiments combining lower concentrations of DDBAC with more realistic light
520 regimes would be required to completely rule out any interaction effects on aquatic biofilms.

521
522

5- Conclusion

524 In this experiment, we demonstrated that DDBAC exposure strongly impacts river biofilms.
525 DDBAC accumulated quickly in biofilms and damaged the photosynthetic material, in turn
526 altering photosynthesis. There was also evidence for an impact on the structure of the
527 biofilm as changes in its taxonomic composition were observed. Indeed, even though the
528 mortality index did not show greater mortality in the exposed diatoms compared with the
529 controls, microscopic observations suggest that a marked number of individuals were
530 strongly impacted on a physiological level (degraded cell content) and were potentially not
531 viable. This hypothesis is supported by the results obtained during the lipidomic analysis,
532 highlighting a strong decrease in the lipid classes associated with thylakoid membranes
533 specific to microalgae. At elevated concentrations, we highlighted striking effects of DDBAC
534 on the aquatic biota. As DDBAC is a common contaminant with multiple domestic uses,
535 complementary research is needed to characterize its impacts at environmentally relevant
536 concentrations.

537 In contrast, ALAN did not lead to any significant change in biofilms, even though the ALAN
538 treatment modified their exposure to DDBAC. In view of the likely increase in DDBAC
539 concentration in urban waters (downstream of WWTPs) where ALAN is often common, it
540 would also be necessary to investigate whether the effects identified in the present study are
541 manifested at environmental concentrations, under more realistic light regimes, in order to
542 reassess the risk posed by DDBAC to aquatic biodiversity.

543
544

Acknowledgements

546
550

References

Abbott, T., Kor-Bicakci, G., Islam, M.S., Eskicioglu, C., 2020. A Review on the Fate of Legacy and Alternative Antimicrobials and Their Metabolites during Wastewater and Sludge Treatment. International Journal of Molecular Sciences 21, 9241. https://doi.org/10.3390/ijms21239241

Amini Khoeyi, Z., Seyfabadi, J., Ramezanpour, Z., 2012. Effect of light intensity and photoperiod on biomass and fatty acid composition of the microalgae, Chlorella vulgaris. Aquacult Int 20, 41–49. https://doi.org/10.1007/s10499-011-9440-1

Arnold, W.A., Blum, A., Branyan, J., Bruton, T.A., Carignan, C.C., Cortopassi, G., et al., 2023. Quaternary Ammonium Compounds: A Chemical Class of Emerging Concern. Environmental Science and Technology 57(20),7645-7665. https://pubs.acs.org/doi/10.1021/acs.est.2c08244

Battin, T.J., Besemer, K., Bengtsson, M.M., Romani, A.M., Packmann, A.I., 2016. The ecology and biogeochemistry of stream biofilms. Nature Reviews Microbiology 14, 251-263.

Blanck, H., Wangberg, S. A.; Molander, S. 1988. Pollution-Induced Community Tolerance—A New Ecotoxicological Tool. Functional Testing of Aquatic Biota for Estimating Hazards of Chemicals. pp. 219–230. doi:10.1520/STP26265S

Bonnineau, C., Artgias, J., Chaumet, B., Dabrin, A., Faburé, J., Ferrari, B.J.D., et al., 2021. Role of Biofilms in Contaminant Bioaccumulation and Trophic Transfer in Aquatic Ecosystems: Current State of Knowledge and Future Challenges. In: de Voogt, P. (eds) Reviews of Environmental Contamination and Toxicology vol 253. Springer, Cham. https://doi.org/10.1007/398_2019_39

Brett, M., Müller-Navarra, D., 1997. The role of highly unsaturated fatty acids in aquatic foodweb processes. Freshwater Biology 38, 483–499. https://doi.org/10.1046/j.1365-2427.1997.00220.x

Chaumet, B., Morin, S., Hourtané, O., Artigas, J., Delest, B., Eon, M., Mazzella, N., 2019. Flow conditions influence diuron toxicokinetics and toxicodynamics in freshwater biofilms. Science of The Total Environment 652, 1242–1251. https://doi.org/10.1016/j.scitotenv.2018.10.265

Chen, Y., Geurts, M., Sjollema, S.B., Kramer, N.I., Hermens, J.L.M., Droge, S.T.J., 2014. Acute toxicity of the cationic surfactant C12-benzalkonium in different bioassays: How test design affects bioavailability and effect concentrations. Environmental Toxicology and Chemistry 33, 606–615. https://doi.org/10.1002/etc.2465

Clara, M., Scharf, S., Scheffknecht, C., Gans, O., 2007. Occurrence of selected surfactants in untreated and treated sewage. Water Research 41, 4339–4348. https://doi.org/10.1016/j.watres.2007.06.027

Demailly, F., Elfeky, I., Malbezin, L., Le Guédard, M., Eon, M., Bessoule, J.-J., Feurtet-Mazel, A., Delmas, F., Mazzella, N., Gonzalez, P., Morin, S., 2019. Impact of diuron and S-metolachlor on the freshwater diatom Gomphonema gracile: Complementarity between fatty acid profiles and different kinds of ecotoxicological impact-endpoints. Science of The Total Environment 688, 960–969. https://doi.org/10.1016/j.scitotenv.2019.06.347

Eich, J., Dürholt, H., Steger-Hartmann, T., Wagner, E., 2000. Specific Detection of Membrane-Toxic Substances with a Conductivity Assay. Ecotoxicology and Environmental Safety 45, 228–235. https://doi.org/10.1006/eesa.1999.1854

Falchi, F., Cinzano, P., Duriscoe, D., Kyba, C.C.M., Elvidge, C.D., Baugh, K., Portnov, B.A., Rybnikova, N.A., Furgoni, R., 2016. The new world atlas of artificial night sky brightness. Science Advances 2, e1600377. https://doi.org/10.1126/sciadv.1600377

Genty, B., Briantais, J.M., Baker, N.R., 1989. The relationship between the quantum yield of photosynthetic electron transport and quenching of chlorophyll fluorescence. Biochimica et Biophysica Acta 990, 87-92. https://doi.org/10.1016/S0304-4165(89)80016-9

Grubisic, M., Singer, G., Bruno, M.C., Grunsven, R.H.A. van, Manfrin, A., Monaghan, M.T., Hölker, F., 2017. Artificial light at night decreases biomass and alters community composition of benthic primary producers in a sub-alpine stream. Limnology and Oceanography 62, 2799–2810. https://doi.org/10.1002/lno.10607

Hora, P.I., Arnold, W.A., 2020. Photochemical fate of quaternary ammonium compounds in river water. Environmental Science: Processes & Impacts 22(6),1368-1381. https://pubs.rsc.org/en/content/articlelanding/2020/em/d0em00086h

Guschina, I.A., Harwood, J.L., 2009. Algal lipids and effect of the environment on their biochemistry. In: Kainz, M., Brett, M., Arts, M. (eds) Lipids in Aquatic Ecosystems. Springer, New York, NY. https://doi.org/10.1007/978-0-387-89366-2_1

Kreuzinger, N., Fuerhacker, M., Grillitsch, B., Scharf, S., Uhl, M., Gans, O., 2007. Methodological approach towards the environmental significance of uncharacterized substances — quaternary ammonium compounds as an example. Desalination 215, 209–222. https://doi.org/10.1016/j.desal.2006.10.036

Laviale, M., Prygiel, J., Lemoine, Y., Courseaux, A., Créach, A. 2009. Stream periphyton photoacclimation response in field conditions: effect of community development and seasonal changes. Journal of Phycology 45, 1072-1082. https://doi.org/10.1111/j.1529-8817.2009.00747.x

Kahrilas, G.A., Blotevogel, J., Stewart, P.S., Borch, T., 2015. Biocides in Hydraulic Fracturing Fluids: A Critical Review of Their Usage, Mobility, Degradation, and Toxicity. Environ. Sci. Technol. 49, 16–32. https://doi.org/10.1021/es503724k

Kim, M., Hatt, J.K., Weigand, M.R., Krishnan, R., Pavlostathis, S.G., Konstantinidis, K.T., 2018. Genomic and Transcriptomic Insights into How Bacteria Withstand High Concentrations of Benzalkonium Chloride Biocides. Appl. Environ. Microbiol. 84. https://doi.org/10.1128/AEM.00197-18

Kreuzinger, N., Fuerhacker, M., Scharf, S., Uhl, M., Gans, O., Grillitsch, B., 2007. Methodological approach towards the environmental significance of uncharacterized substances — quaternary ammonium compounds as an example. Desalination 215, 209–222. https://doi.org/10.1016/j.desal.2006.10.036

Kümmerer, K., Eitel, A., Braun, U., Hubner, P., Daschner, F., Mascart, G., Milandri, M., Reinthaler, F., Verhoef, J., 1997. Analysis of benzalkonium chloride in the effluent from European hospitals by solid-phase extraction and high-performance liquid chromatography with post-column ion-pairing and fluorescence detection. Journal of Chromatography A 774, 281–286. https://doi.org/10.1016/S0021-9673(97)00242-2

Lavorgna, M., Russo, C., D'Abrosca, B., Parrella, A., Isidori, M., 2016. Toxicity and genotoxicity of the quaternary ammonium compound benzalkonium chloride (BAC) using Daphnia magna and Ceriodaphnia dubia as model systems. Environmental Pollution 210, 34–39. https://doi.org/10.1016/j.envpol.2015.11.042

Leal, J.S., González, J.J., Kaiser, K.L.E., Palabrica, V.S., Comelles, F., García, M.T., 1994. On the Toxicity and Biodegradation of Cationic Surfactants Über die Toxizität und den biologischen Abbau kationischer Tenside. Acta hydrochimica et hydrobiologica 22, 13–18. https://doi.org/10.1002/aheh.19940220105

Li-Beisson, Y., Shorrosh, B., Beisson, F., Andersson, M.X., Arondel, V., Bates, P.D., Baud, S., Bird, D., DeBono, A., Durrett, T.P., Franke, R.B., Graham, I.A., Katayama, K., Kelly, A.A., Larson, T.,

643 Markham, J.E., Miquel, M., Molina, I., Nishida, I., Rowland, O., Samuels, L., Schmid, K.M.,
644 Wada, H., Welti, R., Xu, C., Zallot, R., Ohlrogge, J., 2013. Acyl-Lipid Metabolism. arbo.j 2013.
645 https://doi.org/10.1199/tab.0161

646 Longcore, T., Rich, C., 2004. Ecological light pollution. Frontiers in Ecology and the
647 Environment 2, 191–198. https://doi.org/10.1890/1540-9295(2004)002[0191:ELP]2.0.CO;2

648 Lorenzen, C.J., 1967. Determination of chlorophyll and pheo-pigments: Spectrophotometric
649 equations. Limnol. Oceanogr. 12, 343–346. https://doi.org/10.4319/lo.1967.12.2.0343

650 Maggi, E., Serôdio, J., 2020. Artificial Light at Night: A New Challenge in Microphytobenthos
651 Research. Front. Mar. Sci. 7. https://doi.org/10.3389/fmars.2020.00329

652 Martínez-Carballo, E., Sitka, A., González-Barreiro, C., Kreuzinger, N., Fürhacker, M., Scharf, S.,
653 Gans, O., 2007. Determination of selected quaternary ammonium compounds by liquid
654 chromatography with mass spectrometry. Part I. Application to surface, waste and indirect
655 discharge water samples in Austria. Environmental Pollution 145, 489–496.
656 https://doi.org/10.1016/j.envpol.2006.04.033

657 Mazzella, N., Fadhlaoui, M., Moreira, A., Morin, S., 2023a. Molecular species composition of polar lipids
658 from two microalgae *Nitzschia palea* and *Scenedesmus costatus* using HPLC-ESI-MS/MS. PeerJ
659 Analytical Chemistry 5:e27. https://doi.org/10.7717/peerj-achem.27

660 Mazzella, N., Vrba, R., Moreira, A., Creusot, N., Eon, M., Millan-Navarro, D., et al. 2023b. Mixed light
661 photoperiod and biocide pollution affect lipid profiles of periphyton communities in freshwater
662 ecosystems. Journal of Hazardous Materials Advances 12,100378.
663 https://www.sciencedirect.com/science/article/pii/S2772416623001493

664 Mohapatra, S., Xian, J.L.L., Galvez-Rodriguez, A., Ekande, O.S., Drewes, J.E., Gin, K.Y.-H., 2024.
665 Photochemical fate of quaternary ammonium compounds (QACs) and degradation pathways
666 prediction through computational. Journal of Hazardous Materials 465, 133483.
667 https://www.sciencedirect.com/science/article/pii/S030438942400061X

668 Morin, S., Proia, L., Ricart, M., Bonnineau, C., Geiszinger, A., Ricciardi, F., Guasch, H., Romani,
669 A.M., Sabater, S., 2010. Effects of a bactericide on the structure and survival of benthic diatom
670 communities. Vie et Milieu / Life & Environment 60, 109.

671 Neury-Ormanni, J., Vedrenne, J., Wagner, M., Jan, G., Morin, S., 2020. Micro-meiofauna
672 morphofunctional traits linked to trophic activity. Hydrobiologia 847, 2725–2736.
673 https://doi.org/10.1007/s10750-019-04120-0

674 Pandey, L.K., Bergey, E.A., Lyu, J., Park, J., Choi, S., Lee, H., Depuydt, S., Oh, Y.T., Lee, S.M.,
675 Han, T. 2017. The use of diatoms in ecotoxicology and bioassessment: Insights, advances and
676 challenges. Water Research 118, 39-58. https://doi.org/10.1016/j.watres.2017.01.062.

677 Patrauchan, M.A., Oriel, P.J., 2003. Degradation of benzyldimethylalkylammonium chloride by
678 Aeromonas hydrophila sp. K. Journal of Applied Microbiology 94, 266–272.
679 https://doi.org/10.1046/j.1365-2672.2003.01829.x

680 Pérez, P., Fernández, E., Beiras, R., 2009. Toxicity of Benzalkonium Chloride on Monoalgal
681 Cultures and Natural Assemblages of Marine Phytoplankton. Water Air Soil Pollut 201, 319–
682 330. https://doi.org/10.1007/s11270-008-9947-x

683 Perkin, E.K., Hölker, F., Richardson, J.S., Sadler, J.P., Wolter, C., Tockner, K., 2011. The influence
684 of artificial light on stream and riparian ecosystems: questions, challenges, and perspectives.
685 Ecosphere 2, art122. https://doi.org/10.1890/ES11-00241.1

686 Pozo-Antonio, J.S., Sanmartín, P., 2018. Exposure to artificial daylight or UV irradiation (A, B
687 or C) prior to chemical cleaning: an effective combination for removing phototrophs from
688 granite. Biofouling 34, 851–869. https://doi.org/10.1080/08927014.2018.1512103

689   R Core Team (2020). — European Environment Agency [WWW Document], n.d. URL
690   https://www.eea.europa.eu/data-and-maps/indicators/oxygen-consuming-substances-in-
691   rivers/r-development-core-team-2006 (accessed 10.31.22).

692   Rabenau, H.F., Kampf, G., Cinatl, J., Doerr, H.W., 2005. Efficacy of various disinfectants against
693   SARS coronavirus. Journal of Hospital Infection 61, 107–111.
694   https://doi.org/10.1016/j.jhin.2004.12.023

695   Roux, C., Madru, C., Millan-Navarro, D., Jan, G., Mazzella, N., Moreira, A., Vedrenne, J.,
696   Carassou, L., Morin, S., 2024. Impact of urban pollution on freshwater biofilms: Oxidative
697   stress, photosynthesis and lipid responses. Journal of Hazardous Materials 472:164523.
698   https://doi.org/10.1016/j.jhazmat.2024.134523

699   Sakagami, Y., Yokoyama, H., Nishimura, H., Ose, Y., Tashima, T., 1989. Mechanism of resistance
700   to benzalkonium chloride by Pseudomonas aeruginosa. Appl Environ Microbiol 55, 2036–
701   2040.

702   Severina, I.I., Muntyan, M.S., Lewis, K., Skulachev, V.P., 2001. Transfer of Cationic Antibacterial
703   Agents Berberine, Palmatine, and Benzalkonium Through Bimolecular Planar Phospholipid
704   Film and Staphylococcus aureus Membrane. IUBMB Life 52, 321–324.
705   https://doi.org/10.1080/152165401317291183

706   Singh, S.P., Singh, P., 2015. Effect of temperature and light on the growth of algae species: A
707   review. Renew. Sustain. Energy Rev. 50, 431–444. https://doi.org/10.1016/j.rser.2015.05.024

708   Sreevidya, V.S., Lenz, K.A., Svoboda, K.R., Ma, H., 2018. Benzalkonium chloride, benzethonium
709   chloride, and chloroxylenol - Three replacement antimicrobials are more toxic than triclosan
710   and triclocarban in two model organisms. Environmental Pollution 235, 814–824.
711   https://doi.org/10.1016/j.envpol.2017.12.108

712   Sütterlin, H., Alexy, R., Kümmerer, K., 2008. The toxicity of the quaternary ammonium
713   compound benzalkonium chloride alone and in mixtures with other anionic compounds to
714   bacteria in test systems with Vibrio fischeri and Pseudomonas putida. Ecotoxicology and
715   Environmental Safety 71, 498–505. https://doi.org/10.1016/j.ecoenv.2007.12.015

716   Tamminen, M., Spaak, J., Tlili, A., Eggen, R., Stamm, C., Räsänen, K., 2022. Wastewater
717   constituents impact biofilm microbial community in receiving streams. Science of The Total
718   Environment 807, 151080. https://doi.org/10.1016/j.scitotenv.2021.151080

719   Tlili, A., Corcoll, N., Arrhenius, Å., Backhaus, T., Hollender, J., Creusot, N., Wagner, B., Behra,
720   R., 2020. Tolerance patterns in stream biofilms link complex chemical pollution to ecological
721   impacts. Environ. Sci. Technol. 54, 10745–10753. https://doi.org/10.1021/acs.est.0c02975

722   Ugwu, C.U., Aoyagi, H., Uchiyama, H., 2007. Influence of irradiance, dissolved oxygen
723   concentration, and temperature on the growth of Chlorella sorokiniana. Photosynthetica 45,
724   309–311. https://doi.org/10.1007/s11099-007-0052-y

725   United States Environmental Protection Agency 2006. Reregistration eligibility decision for
726   alkyl
727   dimethyl benzyl ammonium chloride. (https://nepis.epa.gov). Accessed on 17 Feb. 2021.

728   US EPA, O., 2020. About List N: Disinfectants for Coronavirus (COVID-19) [WWW Document].
729   URL https://www.epa.gov/coronavirus/about-list-n-disinfectants-coronavirus-covid-19-0
730   (accessed 10.31.22).

731   van Wijk, D., Gyimesi-van den Bos, M., Garttener-Arends, I., Geurts, M., Kamstra, J., Thomas,
732   P., 2009. Bioavailability and detoxification of cationics: I. Algal toxicity of alkyltrimethyl
733   ammonium salts in the presence of suspended sediment and humic acid. Chemosphere 75,
734   303–309. https://doi.org/10.1016/j.chemosphere.2008.12.047

735 Wassenaar, T., Ussery, D., Nielsen, L., Ingmer, H., 2015. Review and phylogenetic analysis of
736 qac genes that reduce susceptibility to quaternary ammonium compounds in Staphylococcus
737 species. European Journal of Microbiology and Immunology 5, 44–61.
738 https://doi.org/10.1556/eujmi-d-14-00038
739 Wood, R.J., Mitrovic, S.M., Kefford, B.J. 2014 Determining the relative sensitivity of benthic
740 diatoms to atrazine using rapid toxicity testing: a novel method. Science of the Total
741 Environment 485-486,421-427. doi: 10.1016/j.scitotenv.2014.03.115.
742 Yang, Z., Geng, L., Wang, W., Zhang, J., 2012. Combined effects of temperature, light intensity,
743 and nitrogen concentration on the growth and polysaccharide content of Microcystis
744 aeruginosa in batch culture. Biochem. Syst. Ecol. 41, 130–135.
745 https://doi.org/10.1016/j.bse.2011.12.015
746 Yin, H., Wang, Lingling, Zeng, G., Wang, Longfei, Li, Y., 2022. The Roles of Different Fractions
747 in Freshwater Biofilms in the Photodegradation of Methyl Orange and Bisphenol A in Aqueous
748 Solutions. Int. J. Environ. Res. Public. Health 19, 12995.
749 https://doi.org/10.3390/ijerph192012995
750 Zhang, C., Cui, F., Zeng, G., Jiang, M., Yang, Z., Yu, Z., Zhu, M., Shen, L., 2015. Quaternary
751 ammonium compounds (QACs): A review on occurrence, fate and toxicity in the environment.
752 Science of The Total Environment 518–519, 352–362.
753 https://doi.org/10.1016/j.scitotenv.2015.03.007
754 Zulu, N.N., Zienkiewicz, K., Vollheyde, K., Feussner, I., 2018. Current trends to comprehend
755 lipid metabolism in diatoms. Progress in Lipid Research 70, 1–16.
756 https://doi.org/10.1016/j.plipres.2018.03.001
757
758
759

Appendices

A- Preliminary experiment

This preliminary experiment aimed to test the sensitivity of our biofilm to dodecyldimethylbenzylammonium (DDBAC) to select a sub-lethal concentration to be used in the main experiment. We ran a dose-response experiment in which we tested nine concentrations ranging between 17.5 µg.L^{-1} and 175 mg.L^{-1} (following a logarithmic increase) for 4 hours. Each concentration was tested twice, one test at a mean light level of 16.86 µmol.s.m^{-2} and the other kept in the dark.

Glass slides (26.5 cm × 6 cm) colonized by biofilms for three months were scraped and the biofilms put into 500 mL of water. For each concentration, we contaminated 1.5 mL of the biofilm solution. After four hours of contamination, we analysed the photosynthetic efficiency of the samples with a Phyto-PAM (see section 2.3).
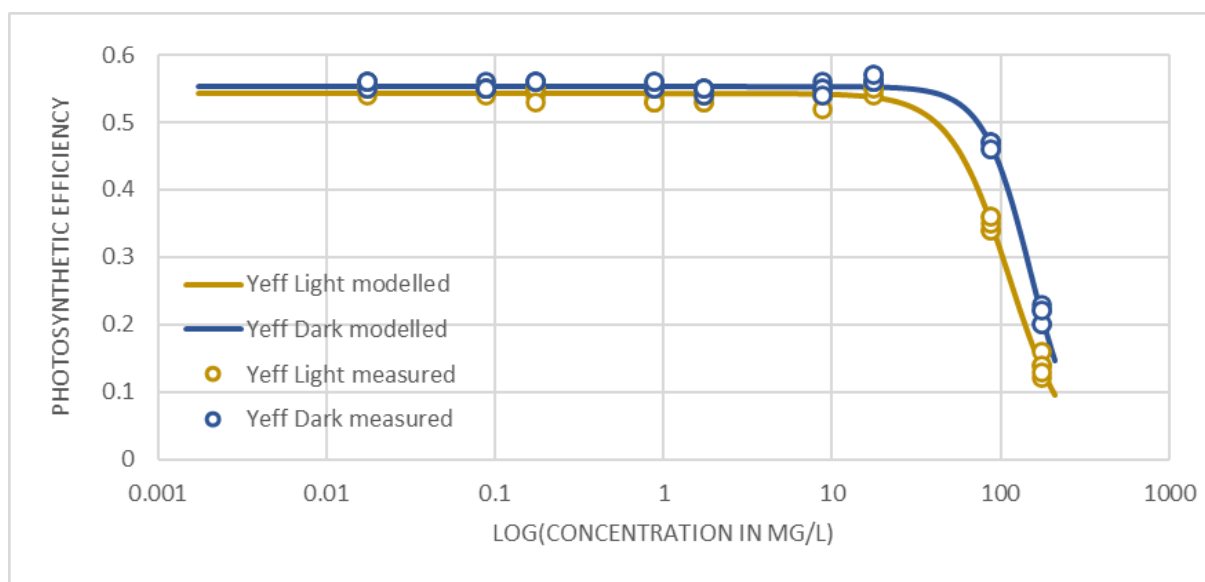
Figure A. Dose-Response curve for photosynthetic efficiency in biofilms exposed to light or dark and increasing DDBAC concentration for 4 hours. Yeff = Photosynthetic efficiency.

The dose-response curve suggests an EC$_{50}$ of 112 ± 3 mg.L^{-1} and a EC$_5$ of 34 ± 3 mg.L^{-1} for photosynthesis inhibition in the biofilm exposed to light. For the biofilm kept in the dark, we found EC$_{50}$ of 151 ± 3 mg.L^{-1} and a EC$_5$ of 58 ± 3 mg.L^{-1}. This result allowed us to choose the concentration of 30 mg.L^{-1} for the 10 days biofilm exposure which is the lowest concentration with a minimum effect on photosynthetic efficiency.

786   **B- Effects of DDBAC on chloroplasts**

787

788

789   **Figure B.1. Chloroplasts of diatoms in non-contaminated biofilm. x400 magnification**

790

791

792   **Figure B.2. Chloroplasts of diatoms in DDBAC contaminated biofilm after 10 days of exposure. x400**
793   **magnification.**

794

795   **C- HPLC gradients for the lipidomic analysis**

796

797   **Table C.1. HPLC gradients for phospholipid and glycolipid analysis.**

798

Time (min)	40 mmol.L^{-1} Ammonium acetate buffer (%)	Acetonitrile (%)
0	5	95
2	5	95
7	30	70
10	30	70
11	5	95
13.7	5	95

799

800   **Table C.2. HPLC gradients for triglyceride analysis.**

801

Time (min)	Solvent A* (%)	Solvent B* (%)
0	50	50
0.3	50	50
5.3	1	99
7.3	1	99
8.3	50	50

9.8	50	50

* Solvent A: solution of acetonitrile/water/40 mmol.L^{-1} ammonium acetate buffer
803 (600/390/10, v/v/v)

804 Solvent B: solution of isopropanol/acetonitrile/1 mol.L^{-1} ammonium acetate buffer
805 (900/90/10, v/v/v)

806

807 **D- Lipid standards**

808 Polar lipid standards were purchased from Avanti Polar Lipids. Quantitations of
809 phosphatidylcholine (PC), phosphatidylethanolamine (PE) and phosphatidylglycerol (PG) were
810 respectively carried out with 1-palmitoyl-2-oleoyl-glycero-3-phosphocholine or PC (16:0/18:1)
811 (850457), 1-palmitoyl-2-oleoyl-sn-glycero-3-phosphoethanolamine or PE (16:0/18:1)
812 (850757), and 1-palmitoyl-2-oleoyl-sn-glycero-3-phospho-(1'-rac-glycerol) or PG (16:0/18:1)
813 (840457).

814 For glycolipids, monogalactosyldiacylglycerol (840523), digalactosyldiacylglycerol (840524)
815 and sulfoquinovosyldiacylglycerol (840525) from plant extracts were used as standards.
816 Quantitation was performed with the following molecular species: MGDG (16:3_18:3) (63% of
817 the total MGDG standard), DGDG (18:3_18:3) (22% of the total MGDG standard), and SQDG
818 (34:3) (78% of the total MGDG standard).

819 1,2-diheptadecanoyl-sn-glycero-3-phosphocholine or PC (2x17:0) (850360) was used as
820 internal standard for PC phospholipids, 1,2-diheptadecanoyl-sn-glycero-3-
821 phosphoethanolamine or PE (2x17:0) (830756) was used as internal standard for PE
822 phospholipids, and 1,2-diheptadecanoyl-sn-glycero-3-phospho-(1'-rac-glycerol) or PG
823 (2x17:0) (830456) was used as internal standard for PG phospholipids, and both MGDG, DGDG
824 and SQDG glycolipids.

825 1,2-dipalmitoyl-sn-glycero-3-O-4'-(N,N,N-trimethyl)-homoserine or DGTS (2x16:0) (857464)
826 was used for the diacylglyceryltrimethylhomo-Ser (DGTS) lipids. 1,2-dipalmitoyl-sn-glycero-3-
827 O-4'-[N,N,N-trimethyl(d9)]-homoserine or DGTS-d9 (2x16:0) (857463) was used as internal
828 standard for DGTS lipids

829 Triglycerides were purchased from Sigma-Aldrich. Tristearin or TAG (3x18:0) (≥99%, T5016)
830 was used as the calibration standard while TAG (3x17:0) (≥99%, T2151) was used as the
831 internal standard.

832

833

834

835 **E- Mass spectrometry parameters for lipid analysis**

836

837 **Table E.1. Mass spectrometry parameters for phospholipid and glycolipid analysis.**

838

	Curtain gas	CAD	IonSpray	Temperature	Ion source gas 1	Ion source gas 2	Declustering potential	Collision energy
MGDG	30 psi	3	-4500 V	450°C	30 psi	60 psi	-61 V	-28 V
DGDG	30 psi	3	-4500 V	450°C	30 psi	60 psi	-61 V	-28 V
SQDG	30 psi	3	-4500 V	450°C	30 psi	60 psi	-126 V	-66 V
PE	30 psi	3	-4500 V	450°C	30 psi	60 psi	-50 V	-50 V
PG	30 psi	3	-4500 V	450°C	30 psi	60 psi	-100 V	-50 V
PC	30 psi	3	-4500 V	450°C	30 psi	60 psi	-100 V	-50 V

839

840

841 **Table E.2. Mass spectrometry parameters for triglyceride analysis.**

	Curtain gas	CAD	IonSpray	Temperature	Ion source gas 1	Ion source gas 2	Declustering potential	Collision energy
Triglycerides	30 psi	3	+5000 V	450°C	30 psi	45 psi	50 V	38 V

842